

# Comparison of Partial Discharge Characteristics for Different Defect Types in SF<sub>6</sub> Gas Insulation System

D.A. Mansour, T. Okusu, K. Nishizawa, H. Kojima, N. Hayakawa, F. Endo and H. Okubo  
Nagoya University  
Furo-cho, Chikusa-ku, Nagoya 464-8603, Japan

**Abstract-** The high reliability, less maintenance and compact size of Gas Insulated Switchgears (GISs) have made them the primary choice for many utilities. However, sometimes insulation defects inside GIS can be a serious threat to safe operation of GIS and can lead to costly disruption of supply. As insulation failure usually starts with partial discharge (PD) activity, this paper investigates the differences in PD characteristics in SF<sub>6</sub> gas among different types of defects. The defect types considered in this study are particles in a gas gap, particles adhered on a spacer surface and spacer/electrode detachment. Different experiments were made for sequential PD measurements using the system of PD-Current Pulse Waveform Analysis (PD-CPWA). The PD phase characteristics, PD pulse number and PD current were analyzed for the different defect types. Also the ratio of voltage increment to phase increment at the next PD pulse appearance ( $\Delta u/\Delta \phi$  pattern) was obtained and compared for each defect type. Experimental results show that correct identification of defects can be achieved based on considered PD characteristics.

## I. INTRODUCTION

Gas insulated switchgears (GISs) have been widely used in the electric power grid with substantial growth since the early seventies. GIS is based on the principle of complete enclosure of all energized parts in a grounded metallic encapsulation insulated with SF<sub>6</sub> gas. Therefore, any defects that are introduced in GIS during manufacturing or operation affect and inhibit the full potential of GIS by affecting the insulation characteristics.

As insulation failure usually starts with partial discharge (PD) activity; several studies have been performed to use PD measurements as a diagnostic method for detecting defects and preventing major insulation breakdown [1, 2]. PD activity in GIS can arise from protrusions on the conductor, free conducting particles, particles fixed on spacer, floating components and spacer defects such as void and detachment as illustrated in Fig. 1 [3]. Metallic particles and spacer detachment were conceived to be the most well-known defects that can exist inside GIS. The extreme field intensity caused by these defects may produce PDs and eventual failure of the system especially under lightning surge condition.

In recent years, the risk assessment of defects on PD monitoring has been eagerly demanded, and many studies have been conducted. For correct risk assessment, it is necessary to know the types of defects reliably. PD-current Pulse Waveform Analysis (PD-CPWA) was developed to provide useful information for this purpose [4].

From this viewpoint, this paper investigates the differences in PD characteristics among the following types of defects:

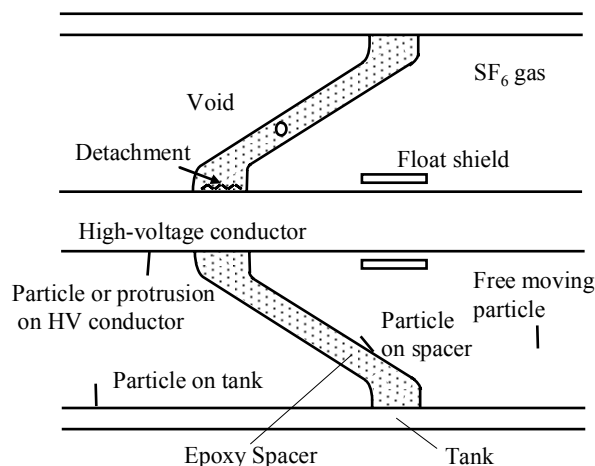


Fig. 1. Example of possible defects in GIS

particles in a gas gap, particles adhered on a spacer surface and spacer/electrode detachment. Consecutive partial discharges usually do not occur in random but in a specific sequence reflecting the physical phenomena of its occurrence [5]. Therefore, the analyses of sequence and number of partial discharge pulses are considered important in determining the local conditions at the defect. In this study, the system of PD-CPWA was used for measurement of PD pulses and the  $\Delta u/\Delta \phi$  pattern was examined as a tool for PD pulse sequence analysis.

## II. EXPERIMENTAL SETUP

Fig. 2 shows the electrode setup for metallic particle defects. Experiments were conducted using parallel plane electrode configuration (gap length: 60 mm) with SF<sub>6</sub> gas at 0.4 MPa. In the first case, an aluminum needle with a section diameter of 0.25 mm and length 5 mm was vertically attached on the grounded electrode. In the second case, a needle with the same size was adhered on a spacer surface. The applied field strength was 2.0 kV<sub>rms</sub>/mm at 60 Hz ac, which is almost equal to the operating conditions of GIS.

The experimental setup used for simulating spacer/electrode detachment consists of a molded plane electrode ( $\epsilon_r = 3.7$ ) connected to high voltage supply and a plane electrode connected to ground as shown in Fig. 3. A rectangular epoxy plate (100 mm × 100 mm × 5 mm) with  $\epsilon_r = 6$  was placed between high voltage and ground electrodes. To provide

detachment, the epoxy plate was separated at a distance 500  $\mu\text{m}$  above and parallel to the ground electrode using a dielectric film. Experiments were conducted in a gas tank filled with  $\text{SF}_6$  at 0.1 MPa. The applied voltage of 60 Hz ac was set at PD inception voltage (PDIV).

For all defect types, PD signals were detected with 50  $\Omega$  resistor. The detected PD signals were fed into the digital oscilloscope (20GS/s, 4GHz) and analyzed by PD-CPWA.

### III. PD INCEPTION AND PROPAGATION CHARACTERISTICS

The partial discharge inception voltage and electric field (PDIV and PDIE) for all defect types are summarized in Table 1 and the typical experimental results for the three defect types

Table 1. PDIV and PDIE for different types of defects

Defect type	PDIV (kV <sub>rms</sub> )	PDIE (kV <sub>rms</sub> /mm)
Particles in a gas gap	57	1
Particles adhered on a spacer surface	48	0.8
Spacer/electrode detachment	12	7.5

mentioned above are shown in Fig. 4. PD was measured for 10 minutes for all cases. From PDIV values, it is evident that for the same particle size, the PDIV for a particle adhered on a spacer surface is lower than PDIV for a particle in a gas gap.

#### A. Phase Characteristics of PD Pulses

In the case of a particle in a gap, many PD pulses appeared broadly around the voltage peak, while in the case of a particle fixed on a spacer surface, several PD pulses per one cycle appeared before the voltage peak. In the detachment case, only several PD pulses appeared in the phase angles of  $(0 - \pi/2)$  rad and  $(\pi - 3\pi/2)$  rad. There were clear differences between PD phase characteristics for the different defects, suggesting that space charge left by previous PD event influences phase occurrence of next PD for each case.

#### B. PD Pulse Number and PD Current

In the case of particle in a gap, the pulse number per second (pps) of negative PD was extremely large. The number was about 10,000 pps at negative PD and about 3000 ~ 4000 pps at positive PD. Though there was fluctuation in the pulse number at negative PD, the pulse number of positive PD was stable. In the case of particle on a spacer, the pulse number was large at the instance of voltage application and decreased to a stable small number in a few minutes. The pulse number of positive PD was extremely larger than that of negative PD.

In the detachment case, The PD pulse number of positive PD was larger than that of negative PD. The pulse number of positive PD increases rapidly at first 60 seconds and after that decrease with time to a stable value. However, the pulse number of negative PD was stable over the 10 minutes. The differences of PD pulse number for different defects are summarized in Fig. 5-(a).

About the average magnitude of PD current, it was found stable for all defect types. Also the average magnitude was almost equal between both polarities. However, each defect type has a different value of average PD current as revealed in Fig. 5-(b). The smallest average PD current is in the case of a particle in a gap. Eventually, it is clear that PD pulse number and PD current differ remarkably among different defect types. Also it is important to observe that the defect type with large number of PD pulses corresponds to small value of average PD current.

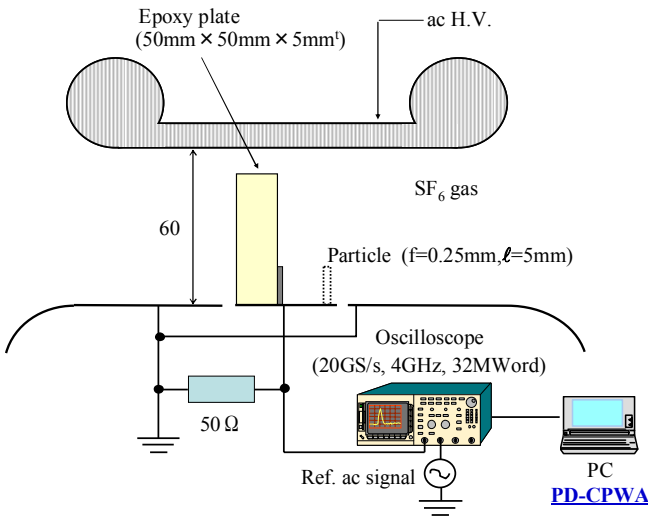
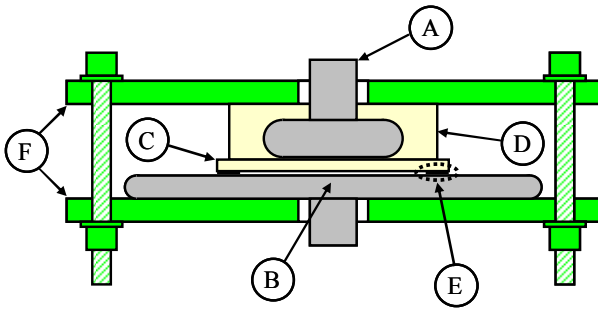
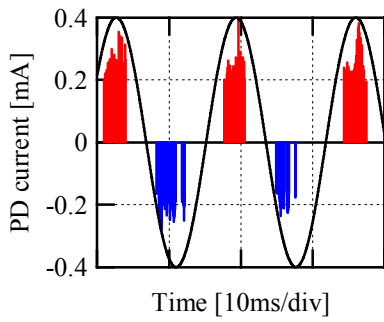


Fig. 2. Electrode setup for metallic particle defects

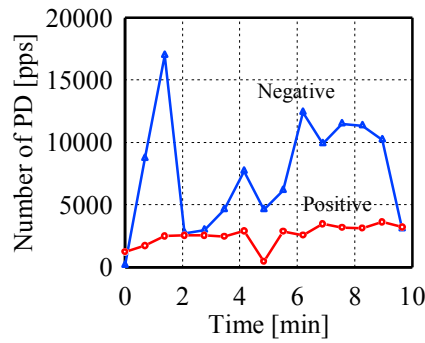


- A: HV molded electrode ( $\Phi 60$  mm)
- B: Ground plain electrode
- C: Epoxy plate (100 mm  $\times$  100 mm  $\times$  t5 mm)
- D: Guard insulation by epoxy ( $\Phi 90$  mm)
- E: Kapton film in  $\mu\text{m}$  thickness
- F: FRP plates ( $\Phi 230$  mm  $\times$  t10 mm)

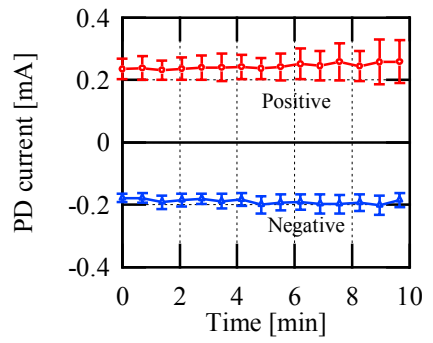
Fig. 3. Electrode configuration for spacer/electrode detachment



(i) Phase characteristics

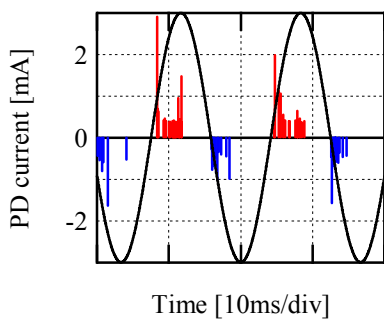


(ii) Temporal change of PD pulse number

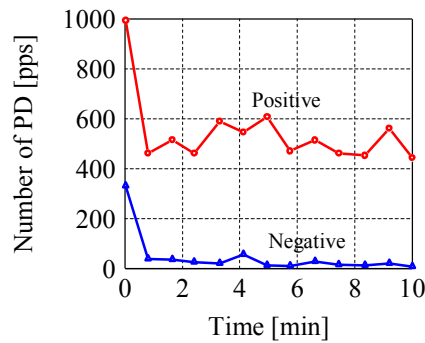


(iii) Average magnitude of PD current

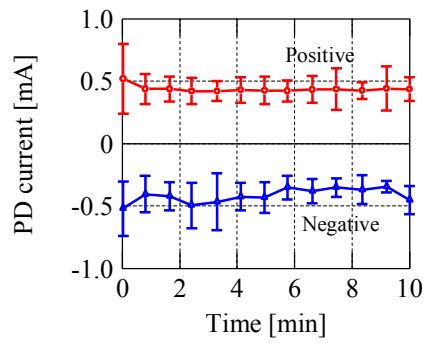
(a) PD characteristics for a particle in a gap (particle length: 5mm)  
[The polarity was expressed as the polarity of a particle tip]



(i) Phase characteristics

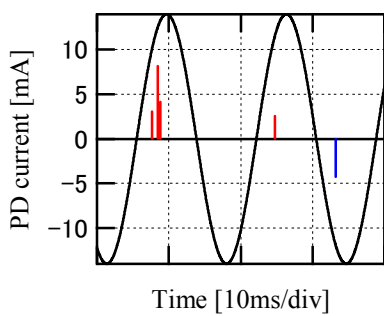


(ii) Temporal change of PD pulse number

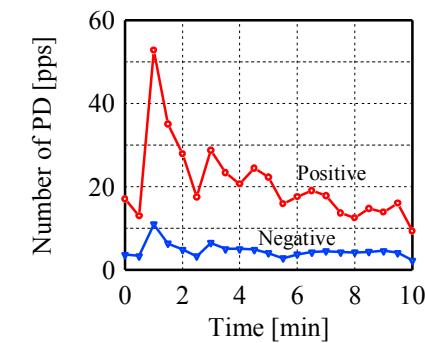


(iii) Average magnitude of PD current

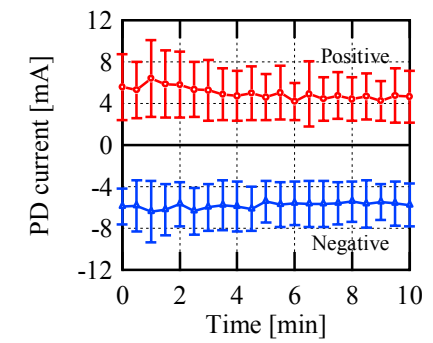
(b) PD characteristics for a particle on a spacer (particle length: 5mm)  
[The polarity was expressed as the polarity of a particle tip]



(i) Phase characteristics



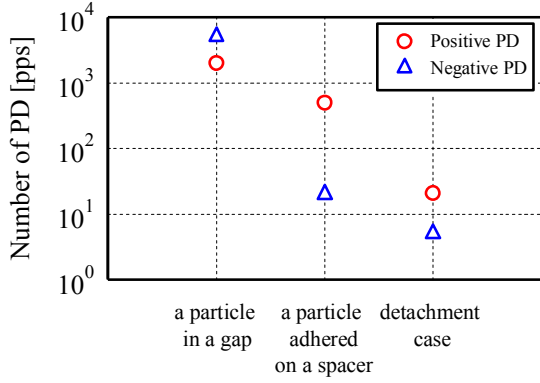
(ii) Temporal change of PD pulse number



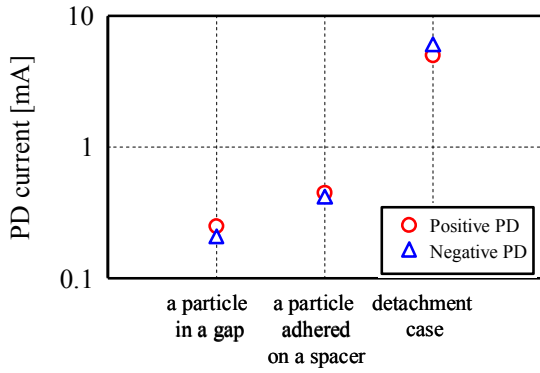
(iii) Average magnitude of PD current

(c) PD characteristics for spacer/electrode detachment (500  $\mu\text{m}$  gap)  
[The polarity was expressed as the polarity of high voltage electrode]

Fig. 4. Experimental results



(a) PD pulse number



(b) PD current

Fig. 5. Effect of particle type on PD characteristics

#### IV. PD PULSE SEQUENCE ANALYSIS

Sequential PD analysis can characterize defects precisely and reflects the underlying physical phenomena within the defect [5]. Each discharge pulse changes the local conditions for the trigger of the next pulse. When there are surface charges deposited by PD, the phase angles of PD pulse appearance are shifted. Thus, the ratio of voltage increment  $\Delta u$  to phase increment  $\Delta\phi$  at the next PD pulse appearance ( $\Delta u/\Delta\phi$  pattern) is used in this study for defect type identification.

##### A. Definition of $\Delta u/\Delta\phi$ Pattern

As illustrated in Fig. 6, In the  $\Delta u/\Delta\phi$  pattern the slope  $m_i = [u(\phi_{i+1})-u(\phi_i)] / [\phi_{i+1}-\phi_i]$  approximates the voltage gradient which is necessary to excite a consecutive PD pulse. When the frequency of the slopes of consecutive PD pulses  $m_i$  and  $m_{i+1}$  are put into a co-occurrence matrix, where  $m_i$  is on the x-axis and  $m_{i+1}$  on the y-axis, a pattern is created which represents a histogram of the PD activities inside the discharging area. The  $\Delta u$  and  $\Delta\phi$  parameters in use can be measured as real quantities and no calibration is needed.

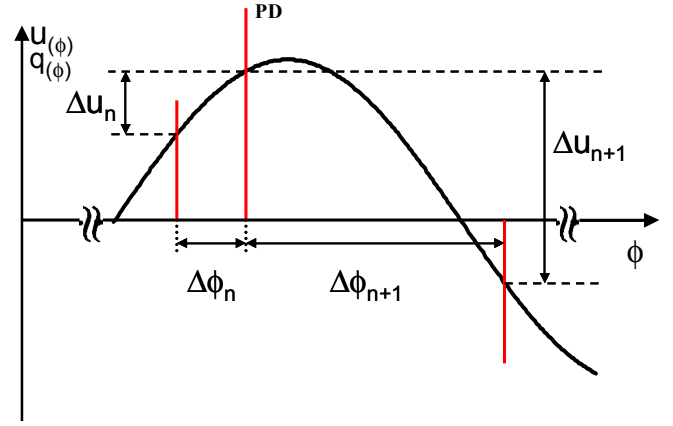


Fig. 6. Definition of  $\Delta u/\Delta\phi$  pattern

##### B. $\Delta u/\Delta\phi$ Pattern for Different Defect Types

The  $\Delta u/\Delta\phi$  pattern of different defects is depicted in Fig. 7. For the case of particles in a gap (Fig. 7a), the pattern exhibited equality between successive  $\Delta u/\Delta\phi$  with some traces in the 2<sup>nd</sup> and 4<sup>th</sup> quadrants resulted from the change of PD pulse between positive and negative half cycles of applied voltage. The points near to the origin represent the PD pulses close to the voltage peak. For the case of particles on a spacer (Fig. 7b), the pattern dispersed over a large area in the four quadrants with certain localization in the 2<sup>nd</sup> and 4<sup>th</sup> quadrants and near the horizontal and vertical axes. The distribution in the 2<sup>nd</sup> and 4<sup>th</sup> quadrants is an indication that for several cases, positive PD pulse is followed by negative PD pulse and vice versa. The points near to the axes are resulted from very small value of  $\Delta u$ , which imply that successive PD pulses with the same polarity usually occur at the same instantaneous voltage. Finally, in the detachment case (Fig. 7c), the points are concentrated around the origin. The cause of this distribution was thought to be the small pps. As the  $\Delta u/\Delta\phi$  pattern is unique to each defect, the type of defect can be identified by analyzing the pattern.

#### VI. CONCLUSION

Partial discharge characteristics were measured and analyzed with a wideband (4 GHz, 20 GS/s) measuring instrument to identify the type of different defect types inside GIS. Different electrode setups were built for simulating possible defect types in GIS. Three types of defects were examined; spacer/electrode detachment, particles in a gas gap and particles adhered on a spacer surface. The results from these investigations primarily demonstrated that PD phase characteristics, PD pulse number and PD current exhibit different tendency for each defect type. This can be useful in distinguishing the defect type, which has advantages for condition monitoring applications. Another important point considered in defect type identification is the pulse sequence analysis using  $\Delta u/\Delta\phi$  pattern. With  $\Delta u/\Delta\phi$  pattern, it was pointed out that each defect type has a unique feature resulting an explicit identification potential for different defects.

REFERENCES

- [1] R. Baumgartner, B. Fruth, W. Lanz and K. Pettersson, "Partial Discharge – Part IX: PD in Gas-Insulated Substations – Fundamental Considerations", IEEE Electr. Insulat. Mag., Vol.7, pp. 5-13, Nov/Dec 1991.
- [2] H. Okubo, Y. Okamoto, N. Hayakawa, T. Hoshino and S. Matsumoto, "Partial Discharge Characteristics by Metallic Particle on Solid Insulator in GIS" International Symposium on High Voltage Engineering, pp.332-335, 2003.
- [3] I. A. Metwally, "Status Review on Partial Discharge Measurement Techniques in Gas-Insulated Switchgear/Lines", J. Electric Power Syst. Res., vol. 69, pp. 25-36, 2004.
- [4] H. Okubo and N. Hayakawa, "A Novel Technique for Partial Discharge and Breakdown Investigation Based on Current Pulse Waveform Analysis", IEEE Trans. Dielectr. Electr. Insulat., vol. 12, pp.736-744, August 2005.
- [5] R. Patsch and F. Berton, "Pulse Sequence Analysis a diagnostic tool based on the physics behind partial discharges" J. Phys. D: Appl. Phys., Vol. 35, pp. 25-32, 2002.

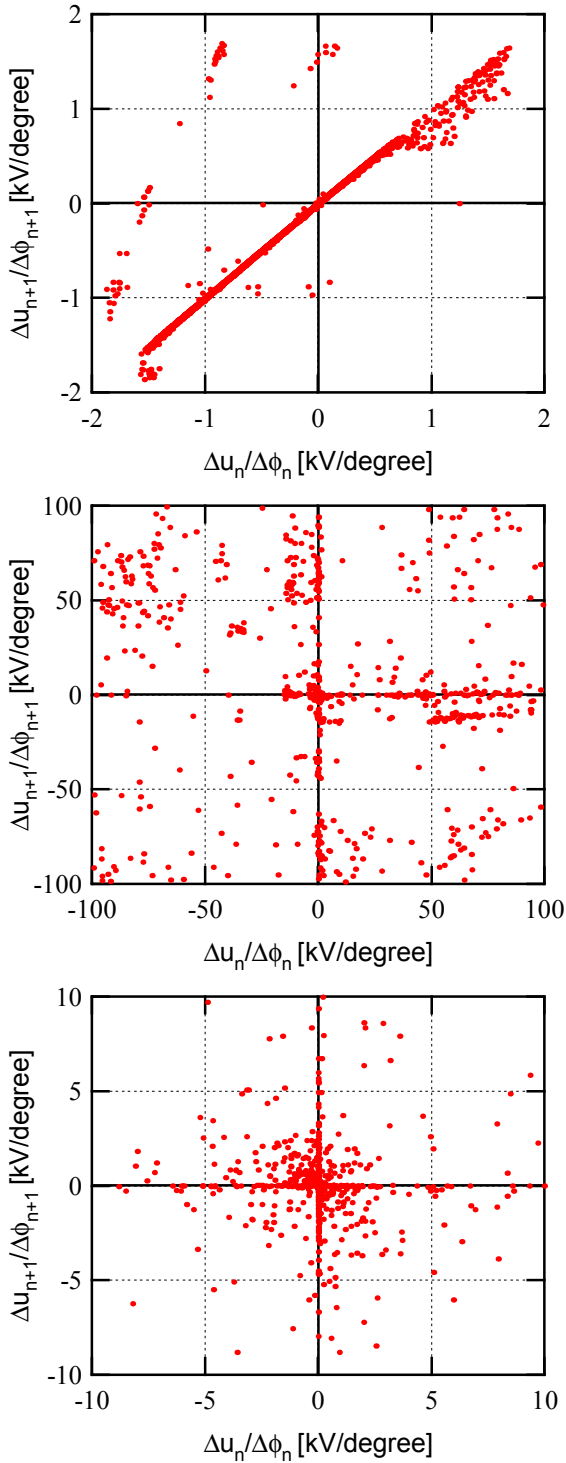


Fig. 7.  $\Delta u / \Delta \phi$  pattern: (a) a particle in a gap. (b) a particle on a spacer. (c) detachment